

Cascaded optical frequency transfer over 500-km fiber link using regenerative amplifier

Xue Deng(邓雪), Dong-Dong Jiao(焦东东), Jie Liu(刘杰), Qi Zang(臧琦), Xiang Zhang(张翔), Dan Wang(王丹), Jing Gao(高静), Rui-Fang Dong(董瑞芳), Tao Liu(刘涛), Shou-Gang Zhang(张首刚)
Citation: Chin. Phys. B . 2020, 29(5): 054205 . **doi:** 10.1088/1674-1056/ab7b4f
Journal homepage: http://cpb.iphy.ac.cn; http://iopscience.iop.org/cpb

What follows is a list of articles you may be interested in

Eigenvalue spectrum analysis for temporal signals of Kerr optical frequency combs based on nonlinear Fourier transform

Jia Wang(王佳), Ai-Guo Sheng(盛爱国), Xin Huang(黄鑫), Rong-Yu Li(李荣玉), Guang-Qiang He(何广强)
Chin. Phys. B . 2020, 29(3): 034207 . **doi:** 10.1088/1674-1056/ab683a

Femtosecond enhancement cavity with kilowatt average power

Jin Zhang(张津), Lin-Qiang Hua(华林强), Shao-Gang Yu(余少刚), Zhong Chen(陈忠), Xiao-Jun Liu(柳晓军)
Chin. Phys. B . 2019, 28(4): 044206 . **doi:** 10.1088/1674-1056/28/4/044206

β-BaB_2O_4 with special cut-angle applied to single crystal cascaded third-harmonic generation

Hong-Kai Ren(任宏凯), Hong-Wei Qi(亓宏伟), Zheng-Ping Wang(王正平), Zhi-Xin Wu(吴志心), Meng-Xia Wang(王梦霞), Yu-Xiang Sun(孙玉祥), Xun Sun(孙洵), Xin-Guang Xu(许心光)
Chin. Phys. B . 2018, 27(11): 114202 . **doi:** 10.1088/1674-1056/27/11/114202

A proposal for the generation of optical frequency comb in temperature insensitive microcavity

Xun Lei(雷勋), Dandan Bian(边丹丹), Shaowu Chen(陈少武)
Chin. Phys. B . 2016, 25(11): 114214 . **doi:** 10.1088/1674-1056/25/11/114214

Monolithic CEO-stabilization scheme-based frequency comb from an octave-spanning laser

Zi-Jiao Yu(于子蛟), Hai-Nian Han(韩海年), Yang Xie(谢阳), Hao Teng(滕浩), Zhao-Hua Wang(王兆华), Zhi-Yi Wei(魏志义)
Chin. Phys. B . 2016, 25(4): 044205 . **doi:** 10.1088/1674-1056/25/4/044205

Cascaded optical frequency transfer over 500-km fiber link using regenerative amplifier*

Xue Deng(邓雪)[1,2,3], Dong-Dong Jiao(焦东东)[1,2,3], Jie Liu(刘杰)[1,3], Qi Zang(臧琦)[1,2,3], Xiang Zhang(张翔)[1,2,3], Dan Wang(王丹)[1,3], Jing Gao(高静)[1,2,3], Rui-Fang Dong(董瑞芳)[1,2,3], Tao Liu(刘涛)[1,3,†], and Shou-Gang Zhang(张首刚)[1,2,3]

[1] *National Time Service Centre, Chinese Academy of Sciences, Xi'an* 710600, *China*
[2] *University of Chinese Academy of Sciences, Beijing* 100049, *China*
[3] *Key Laboratory of Time and Frequency Standards, Chinese Academy of Sciences, Xi'an* 710600, *China*

(Received 11 November 2019; revised manuscript received 13 January 2020; accepted manuscript online 1 March 2020)

We demonstrate a 300-km +200-km cascaded coherent phase transfer via fiber link. The transfer is divided into a 300-km span and a 200-km span with independent phase locking loops, aiming to extend the phase control bandwidth of the whole link. The phase noise and transfer instability of the cascaded transmission are investigated and compared with those in the case of a single-span 500-km transfer. We achieve the transfer instabilities of 1.8×10^{-14} at 1 s, 8.9×10^{-20} at 10^4 s for the 300-km +200-km cascaded transmission, and 2.7×10^{-14} at 1 s for the 500-km single-span transfer.

Keywords: optical frequency, fiber link, transfer

PACS: 42.79.Sz, 06.30.Ft, 42.62.–b **DOI:** 10.1088/1674-1056/ab7b4f

1. Introduction

High-precision optical frequency has various applications in many fields, such as fundamental physics,[1,2] geodesy,[3] metrology,[4,5] *etc*. In recent years, optical clocks have reached and even exceeded 10^{-18} in accuracy and instability,[6,7] allowing high-accuracy measurements in many areas provided that the ultra-stable signal is transferred to the users without quality degradation. So far, fiber link is the only method meeting the requirements for optical clock transmission, which has reached 10^{-20} level in transfer precision for thousand-kilometers dissemination.[8] There are two challenges of optical frequency transfer via fiber links: Doppler shifts introduced by the fiber length fluctuations and optical loss along the fiber. Through detecting the round-trip phase noise and actively modulating the frequency by using an acousto–optic modulator (AOM) in the sender site, the transmitted phase can be stabilized within a propagation-delay-limited bandwidth,[9,10] though out-band phase noise cannot be compensated for. Compared with the single-span transfer, the cascaded transfer improves the bandwidth of phase locking loop (PLL) by separately controlling each shorter segment.[8,11,12] The optical loss is another factor to be overcome, which is not negligible for long-distance fiber link with a typical attenuation of 0.2 dB/km. Optical amplifiers such as bi-directional erbium-doped fiber amplifier (bi-EDFA), fiber Brillouin amplifier (FBA), and Raman amplifier are usually used in the fiber link to compensate for optical loss. As an alternative for the optical amplifier, the optical regeneration is capable of providing a high gain by locking the phase of a local oscillator to the transferred phase[11] and it is usually used in cascaded transfer configuration due to its one-way property. In recent years, many scientific groups have investigated frequency dissemination via fiber links.[13–15] In 2013, an optical frequency transfer over 1840 km was demonstrated in Germany, 20 bi-EDFAs and 2 FBAs were used to compensate for 420-dB optical loss induced by the link, and a transfer instability of 4×10^{-19} at 100 s was achieved with a PLL bandwidth of 27 Hz.[16] The bi-EDFA, as a fairly mature commercial optical amplifier, has played a great role in extending the single-span transfer distance. However, with the extension of single-span transfer distance, the PLL bandwidth is linearly narrowed due to the propagation delay. In 2010, Lopez *et al.* developed a cascaded configuration to transfer optical frequency.[11] A 300-km transfer link was established by connecting two stabilized 150-km fiber link with a regenerative amplifier, obtaining a transfer instability of 5×10^{-20} in 20 h.[11] The cascaded transfer has an advantage in PLL bandwidth over single-span transfer and provides a method for network dissemination. Nevertheless, the direct comparison between the cascaded scheme and single-span scheme has not been demonstrated to our knowledge. Furthermore, the system of controlling the cascaded scheme is more complex with several PLLs in it, and residual phase noise of the last segment may affect the phase detection and stabilization of the next

*Project supported by the National Key Research and Development Program of China (Grant No. 2016YFF0200200), the National Natural Science Foundation of China (Grant Nos. 91636101, 91836301, and 11803041), the West Light Foundation of the Chinese Academy of Sciences (Grant No. XAB2016B47), and the Strategic Priority Research Program of the Chinese Academy of Sciences (Grant No. XDB21000000).

†Corresponding author. E-mail: taoliu@ntsc.ac.cn

© 2020 Chinese Physical Society and IOP Publishing Ltd

segment, and thus increasing the control complicacy. Hence, it is significant to study the phase noise and instability of each segment to further investigate the characteristics of the cascaded transfer.

In this paper, we present a cascaded 300-km +200-km optical frequency transfer by using spooled fiber link. Providing 46-dB gain, a regenerative amplifier is used after 300-km transfer. The phase noise and transfer instability of each span are investigated, so is the dependence of transfer instability of entire link on the segmental instabilities. The 500-km cascaded link reaches a transfer instability of 1.8×10^{-14} at 1 s and 8.9×10^{-20} at 10^4 s. For comparison, we also investigate the coherent phase transfer over a 500-km single-span link. The comparison of PLL bandwidth and phase noise cancellation between the two schemes is conducted. The results show that the single-span configuration possesses a weaker phase noise cancellation and a transfer instability of 2.7×10^{-14} in 1 s. The theoretical relation between the instabilities of unequal segmental cascaded link and single-span link is deduced in the paper, and the experimental results are discussed. This work sets a platform for studying the multi-node optical frequency transfer networks.

2. Optical regeneration

Optical regeneration locks the phase of a local laser to the phase of incoming signal to realize optical amplification, which shows a much narrower amplification bandwidth than bi-EDFA and FBA. Figure 1 shows the schematic diagram of regenerative amplification. Input signal (power 40 nW, linewidth 2 Hz, wavelength 1550.12 nm) is split into two portions by single mode coupler 1 (SMC1) with a ratio of 90 : 10. The 90% portion is injected to the SMC2 for phase detection, while the 10% portion serves as a reference signal. Another input of the SMC2 comes from the local optical oscillator (linewidth 1 kHz, NKT E15, wavelength 1550.12 nm) that has passed through an acousto–optic modulator (AOM). The SMC3 also has a ratio of 90 : 10, the 10% output is sent to SMC2 for heterodyne detection, and the 90% output is launched for use. The heterodyne signal is detected by a photo diode with a bandwidth of 250 MHz. By demodulating the heterodyne signal with a local radio frequency (RF), the phase difference between the input signal and the optical oscillator is derived, then fed into the AOM and piezo-electric transducer (PZT) of the optical oscillator through servo systems. With a large dynamic range (8 GHz), the PZT deals with slow frequency drifts and roughly maintains the frequency difference between the input signal and output signal at a firm value (−160 MHz). The AOM has a much higher response rate and suppresses phase noise with a wide bandwidth (tens kHz bandwidth). Combination of AOM and PZT is able to lock the two lasers with mHz relative frequency fluctuations for several days. The output of the amplification is 16 mW, corresponding to 56-dB gain.

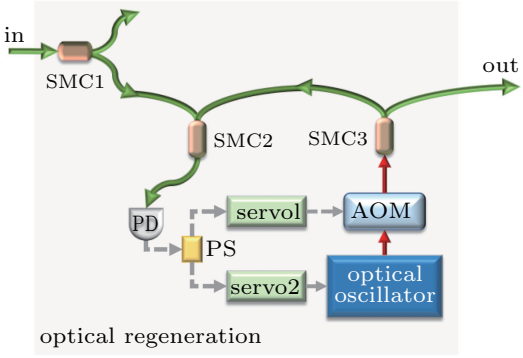


Fig. 1. Schematic graph of optical regeneration based on heterodyne phase locking. SMC: single mode coupler; PD: photo diode; PS: power splitter; AOM: acousto-optic modulator.

To estimate the features of regenerative amplification, the phase noise power spectrum density (PSD) of the regenerative amplifier from 1 Hz to 0.1 MHz is investigated with a fast Fourier transfer (FFT), and the phase noise PSD of the input laser and free-running local oscillator are both studied. All of them are shown in Fig. 2. The free-running local oscillator shows much greater phase noise (black line) than the ultra-stable input laser (red line). Through phase locking, the phase noise of the local oscillator is significantly suppressed within the control bandwidth. The blue line shows close-loop phase noise of the beat-note signal between local oscillator and input laser. For Fourier frequency less than 600 Hz, the phase noise of the regenerative amplification is negligible as it is much lower than that of the input signal. The bump at 7.7 kHz shows the bandwidth of the phase locking loop. For Fourier frequency higher than 7.7 kHz, the regenerative laser shows a phase noise consistent with that of the free-running oscillator. Thus, the regenerative amplifier also plays a role of optical filter with a bandwidth of 7.7 kHz. In addition, the unidirectionality of regenerative amplifier enables the insulation of the back reflections, while the bi-directional EDFA cannot avoid the back reflections nor Rayleigh scatterings which may induce lasing effects.

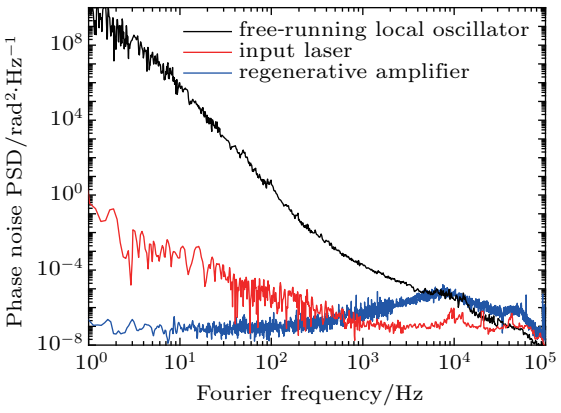


Fig. 2. Plots of phase noise PSD *versus* Fourier frequency for phase noise of the free-running local oscillator (black line), input laser (red line), and regenerative amplifier (blue line).

3. The cascaded 300-km + 200-km optical frequency transfer

A cascaded 500-km coherent phase transfer link via fiber is established, which is constituted by a phase-controlled 300-km link and 200-km link. The optical signal is amplified by the regenerative amplification after 300-km dissemination (the optical gain is 46 dB with 0.35-μW input power and 16-mW output power), then the amplified signal is injected into the next 200-km link. Ten 50-km spooled fibers are comprised of the 300-km + 200-km link with an attenuation of 0.2 dB/km. The schematic diagram of the transfer setup is shown in the following Fig. 3.

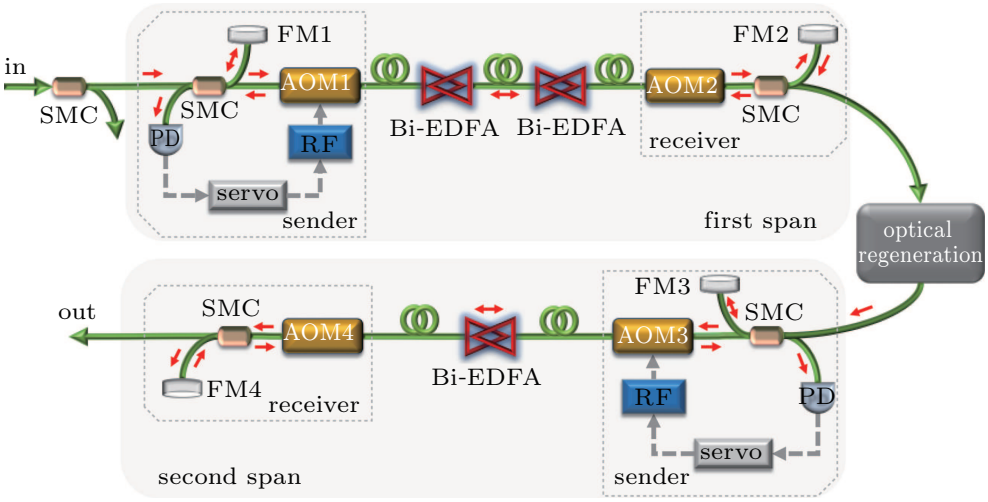


Fig. 3. Setup of cascaded 500-km transfer link. SMC: single mode coupler; PD: photo diode; AOM: acousto–optic modulator; Bi-EDFA: bidirectional EDFA; FM: faraday mirror; RF: radio frequency generator.

Two bi-EDFAs are used in the 300-km link, one EDFA every 100-km transfer, each providing 17-dB gain. One bi-EDFA is used in the 200-km link with a gain of 17 dB. The laser source is an ultra-stable laser (wavelength 1550.12 nm, linewidth 2 Hz) stabilized to an optical cavity by using Pound–Drever–Hall (PDH) method.[17] The laser is split into two parts by a 90 : 10 single mode coupler: the 90% portion is applied to the 300-km transfer while the 10% portion serves as a reference to estimate the transfer precision. The 300-km transfer span consists of a sender, a 300-km fiber link, and a receiver. In the sender site, the major part of laser passes through an x-type coupler with a ratio of 50 : 50, 50% signal is injected into the AOM1 and another 50% signal is sent to the Faraday mirror 1 (FM1). The AOM1 (110 MHz) serves as a phase compensation device of the servo system. The FM1 reflects the signal to the photo diode which will beat with the return signal from the receiver site, thus the double-trip phase noise is detected and compensated for by AOM1. In the receiver site, 90% of the transferred light is sent back to the sender by FM2 along the same path, while the 10% of the transferred light is injected into the regenerative amplifier. After optical regeneration, the optical signal is sent to the second span for cascaded transfer, which has a similar structure to the cascaded transfer for the first span. The phase noise of each span is investigated by measuring the beat-note between the signals before and after each span transfer. The phase noise PSD of the first span and second span are both shown in Fig. 4(a).

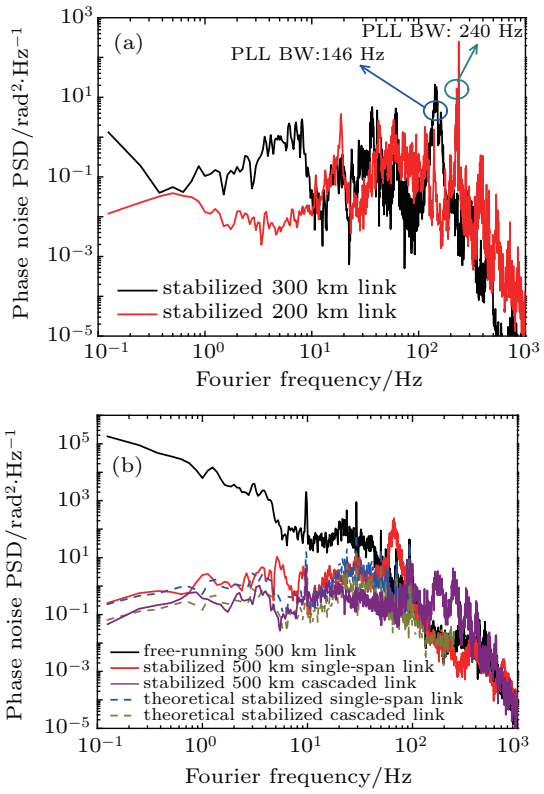


Fig. 4. Plots of phase noise PSD *versus* Fourier frequency of (a) stabilized first span (black line) and stabilized second span (red line) where phase locking bandwidth of each span is shown, (b) unstablized 500-km link (black line), stabilized 500-km cascaded link (purple line), stabilized 500-km single-span link (red line), theoretical stabilized 500-km cascaded link (yellow line), and theoretical stabilized 500-km single-span link (blue line).

In Fig. 4(a), the bump at 146 Hz of the black line indicates that the phase locking loop bandwidth of the 300-km transfer is 146 Hz, and it is 240 Hz for the 200-km span. Phase noise of the 200-km span is measured with both the 300-km span and regenerative amplifier in-lock. According to Ref. [10], the theoretical phase locking loop bandwidth of the Doppler shift cancellation is less than $1/4\tau_0$ due to propagation delay, where τ_0 is the single-trip propagation time. For 300-km link and 200-km link, the theoretical PLL bandwidth are 166 Hz and 250 Hz respectively, which are coincident with the experimental values.

The PLL bandwidth drops to 70 Hz for a single-span 500-km transmission link as shown in Fig. 4(b), meaning a worse phase control than the cascaded scheme. The single-span phase noise cancellation *versus* Fourier frequency is also subjected to τ_0, and the residual phase noise ratio is limited by $(2\pi\tau_0 f)^2/3$, where f is Fourier frequency.[10] Figure 4(b) shows free-running phase noise of 500-km link and stabilized phase noise of cascaded 500-km transfer and single-span 500-km transfer, and it is clear that the cascaded scheme illustrate a better phase noise cancellation. The phase noise cancellation reaches a theoretical limit for both two transfer schemes. Hence, segmental phase control can improve both PLL bandwidth and phase noise suppression ratio compared with the single-span scheme.

To investigate the long-term performance of the 300-km + 200 km link, the out-loop beat-note between the reference signal and the output signal of each segment and the whole cascaded link are measured by a frequency counter (K + K) working on Pi-type mode, owing to the fact that the senders and receivers are located in the same laboratory. And transfer instability *versus* time is evaluated by calculating Allan deviation and modified Allan deviation of the frequency data, which is shown in Fig. 5.

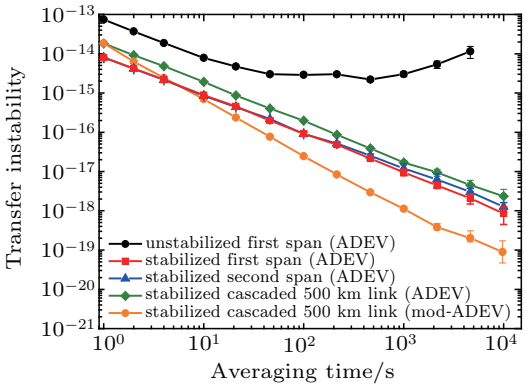


Fig. 5. Transfer instability *versus* averaging time for Allan deviation of unstabilized 300-km link (black line), stabilized 300-km link (red line), stabilized 200-km link (blue line), stabilized 500-km link (green line), and modified Allan deviation of stabilized 500 km (orange line) as well.

The unstabilized 300-km link shows a bad performance at long averaging time due to the Doppler shifts induced by slow temperature perturbations. While the 300-km fiber link is stabilized, a transfer instability of $8.0\times10^{-15}\tau^{-1}$ is achieved, where τ is the averaging time. With the first span stabilized and transferred signal regenerated, transfer instability of the second span is investigated by measuring the beat-note of signals before and after 200-km link, reaching 8.0×10^{-15} s^{-1}. At averaging time from 200 s to 10^4 s, the instability of stabilized 200-km link gradually deviates from the $1/\tau$ slope, which may be caused by asymmetric parts in the second interferometer or cycle slips. In fact, the 200-km link should have shown a better short-term transfer performance than the 300-km link attributed to its shorter distance, nevertheless, the residual phase noise from the first span has a negative effect on phase noise cancellation and the instability evaluation of second-span transfer. The transfer instability of the whole 500-km span is also shown in Fig. 5, and it achieves $1.8\times10^{-14}\tau^{-1}$ expressed as Allan deviation, and approximately $1.8\times10^{-14}\tau^{-3/2}$ expressed as modified Allan deviation, indicating the dominating noise is white phase noise. At 10^4 s of averaging time, the transfer instability of the 500-km link reaches 8.9×10^{-20}. According to $\sigma=\sqrt{\sigma_1^2+\sigma_2^2}$, where σ is the Allan deviation of the whole link and σ_1 and σ_2 are Allan deviations of each span,[18] Allan deviation of the cascaded 500-km link can be deduced from that of 300-km span and 200-km span to be $1.1\times10^{-14}\tau^{-1}$, which is basically in agreement with the experimental result.

4. Comparison between cascaded scheme and single-span scheme

The single-span transfer scheme has a simple structure with a single PLL to compensate for the phase noise of the whole link, yet, PLL bandwidth is exclusively limited by the fiber length, so a thousands of kilometers' transfer leads to tens of hertz's bandwidth. To compare the two transfer schemes, 500-km single-span transfer including a sender, 500-km link and a receiver is also investigated. The fiber link is still comprised of the ten spooled fibers positioned in the same environment. Four bi-EDFAs are used in the 500-km single-span link. The phase noise of the single-span 500-km transfer is shown in Fig. 4(b), and delay-limited phase noise suppression is achieved. The transfer instability of the two transmission schemes is shown in Fig. 6. The stabilized single-span 500-km link obtains a transfer instability of $2.7\times10^{-14}\tau^{-1}$, slightly worse than the transfer instability in the cascaded scheme. The superiority of the cascaded scheme will be further improved with the increase of the number of cascades. Theoretically, it has been proven that cascaded scheme is N times more than single-span scheme in transfer instability for homogeneous link, where N is the number of equal-length cascaded

segments.[19,20] For the unequal segmentation case, we deduce the relation between the instabilities of the stabilized cascaded link and single-span link from phase noise cancellation ratio and the following equation[21]

$$\sigma(\tau) = \sqrt{\int_0^\infty S(f)\sin^4(\pi f\tau)/(\pi f\tau)^2\,\mathrm{d}f}, \tag{1}$$

where $S(f)$ is the PSD of the link. The relation between the instabilities of the stabilized cascaded link and single-span link is expressed as

$$\sigma_{\text{cascade}} = \sqrt{a_1^3 + a_2^3 + \cdots + a_n^3}\,\sigma_{\text{single}}, \tag{2}$$

where a_n is the ratio of n-th length to the total length. In this case, 300-km +200-km cascaded transfer should be 1.9 times superior to the 500-km single-span transmission in transfer instability. The corresponding instability of cascaded transfer should be $1.4\times10^{-14}\tau^{-1}$, though the experimental value is $1.8\times10^{-14}\tau^{-1}$. The mismatch may be caused by phase noise introduced by the asymmetry parts of the interferometers and the influence of residual phase noise of the first span on the phase stabilization of the second span. By carefully setting parameters of the loop filters based on the characteristics of link phase noise, the negative effect of the forward cascade on the later cascade can be reduced to a certain extent. So it is especially important for multi-cascade link to design the loop filters according to phase noise characteristics of each link. To reduce the influence of asymmetry parts of interferometers, temperature control, vibration isolation and acoustic noise reduction are necessary.

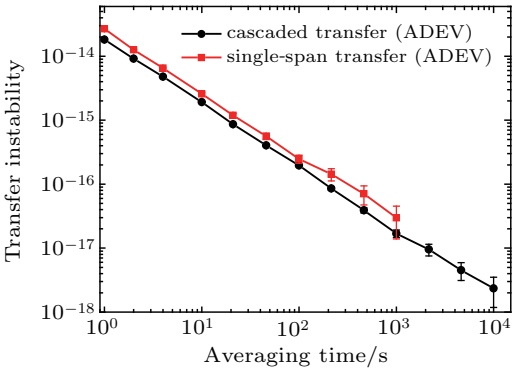


Fig. 6. Allan deviation of single-span 500-km transfer (squares) and cascaded 500-km transfer (circles).

5. Conclusions and perspectives

In this work, a cascaded 300-km +200-km transfer is demonstrated, reaching a transfer instability of 8.9×10^{-20} at 10^4 s by stabilizing each span separately. The phase noise of each span is investigated, and measured PLL bandwidths for the 300-km span and 200-km span are 160 Hz and 240 Hz respectively, consistent with their corresponding theoretical values. The PLL bandwidth for the single-span 500-km link is only 70 Hz. Hence, cascaded transfer scheme can provide preferable phase noise cancellation, which is verified in our work by comparing phase noise cancellations and transfer instabilities of the two schemes. The relation between the instabilities of cascaded link and single-span link is also discussed in the paper. Since the superiority of the cascaded transfer is related to the cascade number, multi-cascaded transfer is a promising method of lengthening distance transfer and noisy links, although complexity of the transmission system will increase at the same time. A challenge of the cascaded transfer is the residual phase noise of the last cascade transferring to the next cascade, which needs to set suitable loop filter for each link. And it is necessary to reduce the asymmetry parts of the interferometers by shortening the length of fibers and employing temperature control and vibration isolation. In future, we will work on multi-segment cascaded transfer and investigate the characteristics of phase noise suppression of each span for high-precision long-distance optical frequency transfer.

References

[1] Parthey Ch G, Matveev A, Alnis J, Bernhardt B, Beyer A, Holzwarth R, Maistrou A, Pohl R, Predehl K, Udem Th, Wilken T, Kolachevsky N, Abgrall M, Rovera D, Salomon Ch, Laurent Ph and Hänsch Th W 2011 *Phys. Rev. Lett.* **107** 203001

[2] Schiller S, Tino G M, Gill P, Salomon C, Sterr U, Peik E, Nevsky A, Görlitz A, Svehla D, Ferrari G, Poli N, Lusanna L, Klein H, Margolis H and Lemonde P 2009 *Exp. Astron.* **23** 573

[3] Grotti J, Koller S, Vogt S, *et al.* 2018 *Nat. Phys.* **14** 437

[4] Chou C W, Hume D B, Rosenband T and Wineland D J 2010 *Science* **329** 1630

[5] Riehle F 2017 *Nat. Photon.* **11** 25

[6] Bloom B J, Nicholson T L, Williams J R, Campbell S L, Bishof M, Zhang X, Zhang W, Bromley S L and Ye J 2014 *Nature* **506** 71

[7] Campbell S L, Hutson R B, Marti G E, Goban A, Darkwah Oppong N, McNally R L, Sonderhouse L, Robinson J M, Zhang W, Bloom B J and Ye J 2017 *Science* **358** 90

[8] Chiodo N, Quintin, Stefani F, Wiotte F, Camisard E, Chardonnet Ch, Santarelli G, Klein A A, Pottie P E and Lopez O 2015 *Opt. Express* **23** 33927

[9] Ma L S, Jungner P, Ye J and Hall J L 1994 *Opt. Lett.* **19** 1777

[10] Newbury N R, Williams P A and Swann W C 2007 *Opt. Lett.* **32** 3056

[11] Lopez O, Chiodo N, Stefani F, Wiotte F, Quintin N, Bercy A, Chardonnet Ch, Santarelli G, Pottie P E and Klein A A 2010 *Opt. Express* **18** 16849

[12] Ma C Q, Wu L F, JiangY Y, Yu H F, Bi Z Y and Ma L S 2015 *Appl. Phys. Lett.* **107** 261109

[13] Deng X, Liu J, Jiao D D, Gao J, Zang Q, Xu G J, Dong R F, Liu T and Zhang S G 2016 *Chin. Phys. Lett.* **33** 114202

[14] Grosche G, Terra O, Predehl K, Holzwarth R, Lipphardt B, Vogt F, Sterr U and Schnatz H 2009 *Opt. Lett.* **34** 2270

[15] Cheng N, Chen W, Liu Q, Xu D, Yang F, Gui Y Z and Cai H W 2016 *Chin. Phys. B* **25** 014206

[16] Droste S, Predehl K, Hänsch T W, Udem Th, Holzwarth R, Raupach S M F, Ozimek F, Schnatz H and Grosche G 2013 *Phys. Rev. Lett.* **111** 110801

[17] Jiao D D, Gao J, Liu J, Deng X, Xu G J, Chen J, Dong R F, Liu T and Zhang Sh G 2015 *Acta Phys. Sin.* **64** 190601 (in Chinese)

[18] Deng X, Liu J, Zang Q, Jiao D D, Gao J, Zhang X, Wang D, Dong R F and Liu T 2018 *Appl. Opt.* **57** 9620

[19] Musha M, Hong F L, Nakagawa K and Ueda K 2008 *Opt. Express* **16** 16459

[20] Fujieda M, Kumagai M and Nagano S 2010 *IEEE Trans. Ultrason. Ferroelectr. Freq. Control* **57** 168

[21] Cutler L and Searle C 1966 *Proc. IEEE* **54** 136